受入
91-11-94
高エ研図書室

EUROPEAN ORGANIZATION FOR NUCLEAR RESEARCH

CERN-PPE/91-163
30 September, 1991

An Improved Determination of the Ratio of W and Z Masses at the CERN $\bar{p}p$ Collider

The UA2 Collaboration

Bern - Cambridge - CERN - Dortmund - Heidelberg - Melbourne -
Milano - Orsay (LAL) - Pavia - Perugia - Pisa - Saclay (CEN)

J. Alitti[12], G. Ambrosini[9], R. Ansari[8], D. Autiero[11], P. Bareyre[12], I. A. Bertram[6], G. Blaylock[3,a], P. Bonamy[12], K. Borer[1], M. Bourliaud[12], D. Buskulic[8], G. Carboni[11], D. Cavalli[7], V. Cavasinni[11], P. Cenci[10], J. C. Chollet[8], C. Conta[9], G. Costa[7], F. Costantini[11], L. Cozzi[7], A. Cravero[7], M. Curatolo[11], A. Dell'Acqua[9], T. DelPrete[11], R. S. DeWolf[2], L. DiLella[3], Y. Ducros[12], G. F. Egan[6], K. F. Einsweiler[3,b], B. Esposito[11], L. Fayard[8], A. Federspiel[1], R. Ferrari[9], M. Fraternali[9,c], D. Froidevaux[3], G. Fumagalli[9], J. M. Gaillard[8], F. Gianotti[7], O. Gildemeister[3], C. Gössling[4], V. G. Goggi[9], S. Grünendahl[5], K. Hara[1,d], S. Hellman[3], J. Hřivnáč[3], H. Hufnagel[4], E. Hugentobler[1], K. Hultqvist[3,e], E. Iacopini[11,f], J. Incandela[7], K. Jakobs[3], P. Jenni[3], E. E. Kluge[5], N. Kurz[5], S. Lami[11], P. Lariccia[10], M. Lefebvre[3], L. Linssen[3], M. Livan[9,g], P. Lubrano[3,10], C. Magneville[12], L. Mandelli[7], L. Mapelli[3], M. Mazzanti[7], K. Meier[3,h], B. Merkel[8], J. P. Meyer[12], M. Moniez[8], R. Moning[1], M. Morganti[11,i], L. Müller[1], D. J. Munday[2], M. Nessi[3], F. Nessi-Tedaldi[3], C. Onions[3], T. Pal[1], M. A. Parker[2], G. Parrour[8], F. Pastore[9], E. Pennacchio[9], J. M. Pentney[3], M. Pepe[3], L. Perini[7,c], C. Petridou[11], P. Petroff[8], H. Plothow-Besch[3], G. Polesello[3,9], A. Poppleton[3], K. Pretzl[1], M. Primavera[11,j], M. Punturo[10], J. P. Repellin[8], A. Rimoldi[9], M. Sacchi[9], P. Scampoli[10], J. Schacher[1], B. Schmidt[4], V. Šimák[3], S. L. Singh[2], V. Sondermann[4], R. Spiwoks[4], S. Stapnes[3], C. Talamonti[10], F. Tondini[10], S. N. Tovey[6], E. Tsesmelis[4], G. Unal[8], M. Valdata-Nappi[11,j], V. Vercesi[9], A. R. Weidberg[3,k], P. S. Wells[2,ℓ], T. O. White[2], D. R. Wood[8], S. A. Wotton[2,ℓ], H. Zaccone[12], A. Zylberstejn[12]

(submitted to Phys. Lett. B)

Abstract

The W and Z bosons masses, m_W and m_Z, are measured using samples of $W \to e\nu$ and $Z \to e^+e^-$ decays observed in $\overline{p}p$ collisions at $\sqrt{s} = 630$ GeV. The ratio is found to be $m_W/m_Z = 0.8813 \pm 0.0036 \pm 0.0019$. This gives a value $\sin^2\theta_W = 0.2234 \pm 0.0064 \pm 0.0033$, and in combination with precise m_Z measurements from LEP yields $m_W = 80.35 \pm 0.33 \pm 0.17$ GeV. This result is in good agreement with other experiments, and with the Standard Model for a top quark mass lighter than 250 GeV.

[1]Laboratorium für Hochenergiephysik, Universität Bern, Sidlerstraße 5, 3012 Bern, Switzerland
[2]Cavendish Laboratory, University of Cambridge, Cambridge, CB3 0HE, UK
[3]CERN, 1211 Geneva 23, Switzerland
[4]Lehrstuhl für Exp. Physik IV, Universität Dortmund, 4600 Dortmund, FRG
[5]Institut für Hochenergiephysik der Universität Heidelberg, Schröderstraße 90, 6900 Heidelberg, FRG
[6]School of Physics, University of Melbourne, Parkville 3052, Australia
[7]Dipartimento di Fisica dell'Università di Milano and Sezione INFN Milano, 20133 Milano, Italy
[8]Laboratoire de l'Accélérateur Linéaire, Université de Paris-Sud, 91405 Orsay, France
[9]Dipartimento di Fisica Nucleare e Teorica, Università di Pavia and INFN, Sezione di Pavia, Via Bassi 6, 27100 Pavia, Italy
[10]Dipartimento di Fisica dell'Università di Perugia and INFN, Sezione di Perugia, Via Pascoli, 06100 Perugia, Italy
[11]Dipartimento di Fisica dell'Università di Pisa and INFN Sezione di Pisa, Via Livornese, S. Piero a Grado, 56100 Pisa, Italy
[12]Centre d'Etudes Nucléaires de Saclay, 91191 Gif-sur-Yvette Cedex, France
a) Now at University of California, Santa Cruz, USA
b) Now at Lawrence Berkeley Laboratory, Berkeley, California, USA
c) Now at Istituto di Fisica, Università di Palermo, Italy
d) Now at University of Tsukuba, Tsukuba, Ibaraki 305, Japan
e) Now at University of Stockholm, Stockholm, Sweden
f) Also at Scuola Normale Superiore, Pisa, Italy
g) Now at Dipartimento di Fisica, Università di Cagliari, Italy
h) Now at Deutsches Elektronen Synchrotron, Hamburg, FRG
i) Now at Dipartimento di Fisica e INFN di Bologna, Università di Bologna, Italy
j) Now at Dipartimento di Fisica dell'Università della Calabria e gruppo INFN, Cosenza, Italy
k) Now at Nuclear Physics Laboratory, University of Oxford, Oxford, UK
ℓ) Now at CERN, Geneva, Switzerland

1 Introduction

In 1990, new measurements of the W mass (m_W) were published by the UA2 [1] and CDF [2] collaborations. The precision of these determinations far exceeded that of earlier measurements. The W mass continues to be a subject of great interest in testing the Standard Model, and thus UA2 has combined the data from the 1990 run of the CERN $\bar{p}p$ collider with the data set of the previous publication to obtain an improved measurement of the W mass, based on a total integrated luminosity of 13 pb^{-1}.

The method used to determine m_W follows closely that used in the previous UA2 measurement [1]. The W mass is measured from fits to transverse mass and momentum spectra in $W \rightarrow e\nu$ decays, while the Z mass (m_Z) is determined concurrently from the $Z \rightarrow e^+e^-$ decays. The calibration scale errors largely cancel in the ratio of the two masses, so a precise value of m_W is obtained by rescaling the ratio with the m_Z value from LEP.

The present analysis has benefitted doubly from the increase in statistics. The statistical uncertainty on m_W/m_Z has decreased, and in addition the larger sample of $Z \rightarrow e^+e^-$ events has been used to study the detector response in greater detail and has thereby made possible a reduction in the systematic errors in the $W \rightarrow e\nu$ event reconstruction.

2 Event Selection and Reconstruction

The data were collected from 1988 to 1990 at the CERN $\bar{p}p$ collider at an energy of $\sqrt{s} = 630$ GeV. After removing events where not all of the detector elements used in this analysis were functioning, the useful integrated luminosity is 13.0 ± 0.7 pb^{-1}. Requirements are imposed in order to select events where $\bar{p}p \rightarrow W + X$, $W \rightarrow e\nu$ or $\bar{p}p \rightarrow Z + X$, $Z \rightarrow e^+e^-$. The upgraded UA2 detector is described in the accompanying letter [3].

2.1 Electron Identification

A standard electron candidate must have a track reconstructed in the tracking detectors which points to an electromagnetic cluster in the calorimeter. The track must originate from a reconstructed vertex which is not displaced more than 250 mm along the beam direction from the centre of the detector. The lateral and longitudinal profile of the shower in the calorimeter is required to be consistent with that expected from an electron incident along the track trajectory as measured in test beams. Furthermore, a preshower cluster must be reconstructed which is consistent with the position of the electron candidate track. In addition, a set of looser electron cuts is defined for the region covered by the central calorimeter, in order to recover electrons for which either the track or the preshower cluster is not correctly reconstructed by the standard pattern recognition algorithms [4].

The detected energy is summed in a small number (typically two or three) of calorimeter cells ("core" cells) which are assigned to the electron. Energy corrections are applied according to the precise electron direction and impact point in the calorimeter based on data obtained from 40 GeV test beam electrons. The corrected energy is used together with the direction given by the tracking detectors to define the electron momentum, $\vec{p}^{\,e}$. The program for maintaining the calibration of the calorimeters described in ref. [1] has been continued

with periodic ^{60}Co source measurements and test beam calibrations of representative modules preceding and following the 1990 running period. In this way, the overall scale of the energy calibration for electrons is controlled to the level of 1% for the central (non-edge) cells.

2.2 Neutrino Identification

The presence of neutrinos in $W \to e\nu$ decays is deduced by measuring the electron energy and the energies of the particles (generally hadrons) recoiling against the W. The missing transverse momentum ($\not\!\!p_T$) is attributed to the undetected neutrino:

$$\vec{p}_T^{\,\nu} \equiv \vec{\not\!\!p}_T = -\vec{p}_T^{\,e} - \vec{p}_T^{\,had}. \tag{1}$$

Here, $\vec{p}_T^{\,e}$ is the reconstructed transverse momentum of the electron candidate and $\vec{p}_T^{\,had}$ is the total transverse momentum of the recoil particles, calculated as

$$\vec{p}_T^{\,had} = \left(\sum E_{cell}\hat{v}_{cell}\right)_T, \tag{2}$$

where $\hat{v}_{cell}$ is a unit vector from the interaction vertex to the centre of a calorimeter cell, E_{cell} is the energy in that cell, and the sum extends over all cells in the calorimeter ($-3 < \eta < 3$) excluding the cells assigned to the electron.

2.3 W Selection Requirements

For the W mass measurement, most of the statistical information comes from events with the electron in the central calorimeter region. This arises from the fact that, due to kinematics, the p_T^e and p_T^ν distributions are much flatter in the forward acceptance regions than in the central region where they peak at about half the W mass. Therefore, this analysis uses only W events in which the electron is in the central calorimeter. Additional fiducial cuts are applied so that the edge cells and the cell borders (0.5° in ϕ and 5 mm in $r\theta$) are excluded in order to obtain high quality energy reconstruction.

The electron must pass the standard identification cuts and have transverse momentum greater than 20 GeV. The neutrino transverse momentum reconstructed in each event must exceed 20 GeV. The transverse mass, m_T, is required to be between 40 GeV and 120 GeV, where $m_T = \sqrt{2p_T^e p_T^\nu(1 - cos\phi^{e\nu})}$ and $\phi^{e\nu}$ is the azimuthal separation between the measured electron and neutrino directions. In addition, the requirement $p_T^W < 20$ GeV is imposed because the p_T^ν resolution is degraded in events with large amounts of hadronic energy. This leaves 2065 events, which are predominantly $W \to e\nu$ events with a 3.8% contribution from the process $W \to \tau\nu$, $\tau \to e\nu\bar{\nu}$, and a negligible QCD background (< 1%) [4].

2.4 Z Selection Requirements

In selecting the samples for the Z mass determination, it is important that the energy scale in the mass measurement comes from the same fiducial volume as defined for the W events. In this way, there is maximal cancellation of the dominant calibration errors in computing the ratio m_W/m_Z. In a first Z sample, both electron candidates are required

to be in the fiducial volume of the central calorimeter. The mass of the electron candidate pair (m_{ee}) is calculated from the corrected momenta of the electrons, and it is required to be between 70 and 120 GeV. This yields a sample of 95 events.

A second independent Z sample is obtained as described in ref. [1]. One electron is required to be in the central fiducial volume while the other one must be outside, either in the forward or edge region or in the cell borders of the central calorimeter. The mass is then calculated by rescaling the momentum of the non-fiducial electron until the total event momentum balances along the ξ axis, where ξ is the outer bisector of the angle between the two electrons in the transverse plane (see inset in Fig. 3). By this procedure, the energy scale of the central calorimeter is transferred to the second electron. This "p_T-constrained" mass is required to be between 70 and 120 GeV, yielding a sample of 156 events. This sample has poorer mass resolution than the central Z sample, but with the larger number of events it makes a significant contribution to the Z mass measurement.

For both Z samples, at least one electron is required to satisfy the standard electron identification cuts, while the other may pass the looser cuts. The background from QCD two-jet events is estimated to be $< 1\%$ [3].

3 Mass fits

3.1 Z Mass fits

The fits to m_Z are shown in Fig. 1. The function

$$f(m_{ee}, \sigma, m_Z, \Gamma_Z) \propto \int dm' \frac{m'^2 e^{-\beta m'}}{(m'^2 - {m_Z}^2)^2 + m'^4 \Gamma_Z^2 / {m_Z}^2} e^{-(m_{ee}-m')^2/2\sigma^2} \qquad (3)$$

is used as the probability density function in a maximum likelihood fit. The function f combines a general relativistic Breit-Wigner resonance shape [5] with a term representing the parton luminosity ($e^{-\beta m'}$) and a convolution with the detector resolution σ for the event considered. The results of the m_Z fits are shown in Table 1. The fits are done both with the width Γ_Z left as a free parameter, and with Γ_Z fixed to the Standard Model value of 2.5 GeV. The fitted widths are in agreement with the Standard Model value. The mass values are rather insensitive to the width, and the final result is taken from the fits with the width fixed.

The function f does not take into account the effect of radiative decays or of the underlying event. A fraction of the sample comes from decays $Z \to e^+e^-\gamma$ and the photon is not included in m_{ee}, so the average reconstructed mass is lowered by $\sim$190 MeV. Meanwhile, particles from the underlying event can contribute energy to the calorimeter cells used to determine the electron momenta, thus increasing m_{ee} by an average of $\sim$250 MeV. A net correction of -60 MeV is added to the fitted mass values to compensate for these effects. The calculation of these effects and their uncertainties are discussed in the context of systematic errors (see Section 4). The results from the two samples of Z events are in good agreement and the combination gives $m_Z = 91.74 \pm 0.28$ GeV (statistical error only) after these corrections are applied.

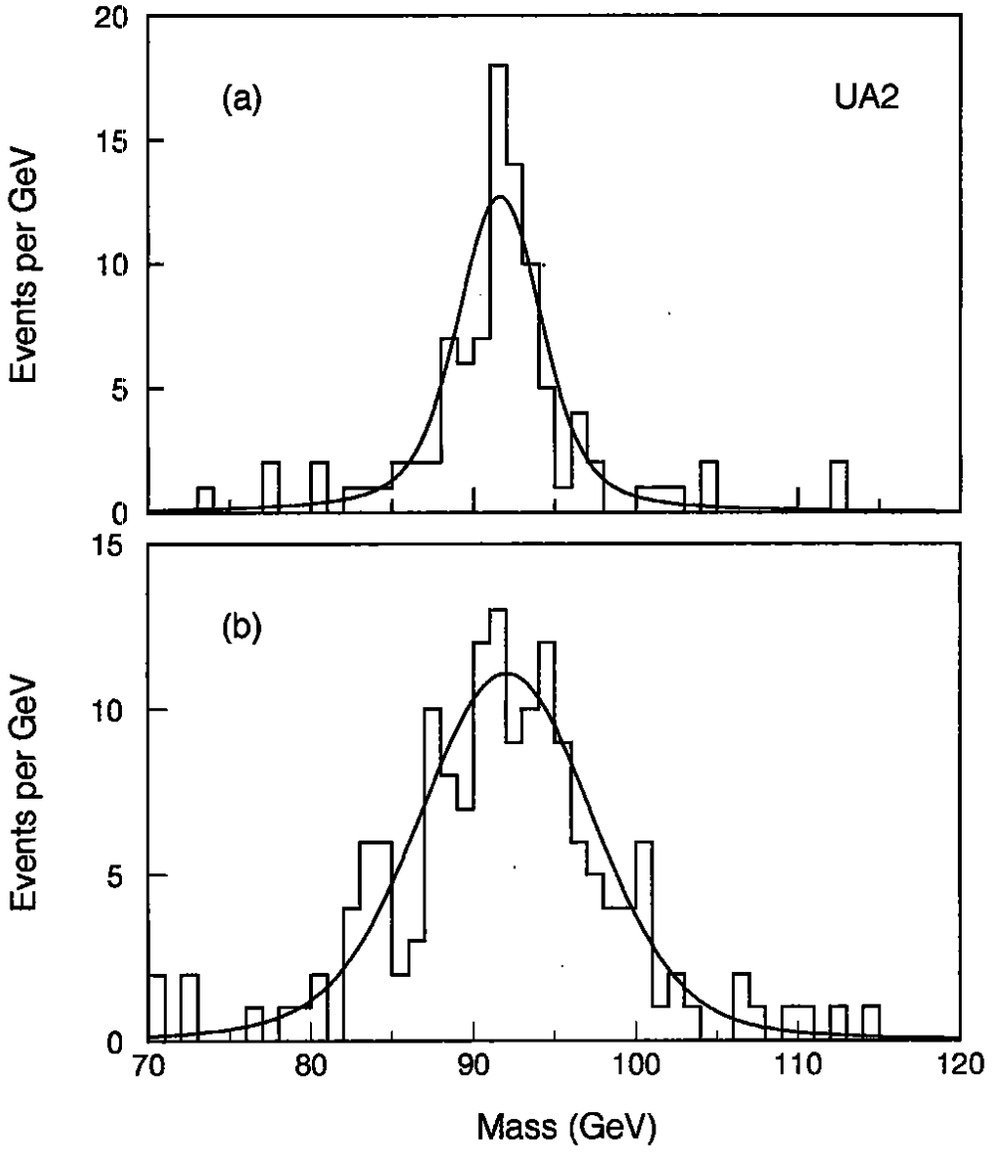

Figure 1: Fits for m_Z to (a) the central sample and (b) the pt-constrained sample. The curves show the fits, while the histograms show the data.

Table 1: Results of m_Z fits (statistical errors only)

	m_Z(GeV)	Γ_Z(GeV)
central	91.65 ± 0.34	2.5 (fixed)
sample	91.67 ± 0.37	3.2 ± 0.8
p_T-constrained	92.10 ± 0.48	2.5 (fixed)
sample	92.15 ± 0.52	3.8 ± 1.1

3.2 W Mass fits

Since the longitudinal momentum of the neutrino is not measured, the W mass must be obtained by fitting to a transverse kinematical variable such as p_T^e, p_T^ν, or m_T. There are no simple analytical forms for these distributions, so the maximum likelihood fits are performed with sets of numerical probability density functions (*pdf*'s). In order to obtain these *pdf*'s, a simple Monte Carlo simulation is used which generates W bosons, forces them to decay into electron and neutrino(s) (either $W \to e\nu$ or $W \to \tau\nu$, $\tau \to e\nu\bar{\nu}$), and models the detector response. For each mass and width the events are given appropriate weights according to the general relativistic Breit-Wigner resonance shape. The rapidity distribution of the W bosons is determined by the choice of structure functions, and the p_T distribution is generated according to the spectrum derived from the study of Z events (see below). Each electron is followed into the calorimeter and smearing is applied to the energy and direction to account for the measurement errors. The energy resolution, which depends on the impact point and cell type, is obtained from look-up tables based on test beam data (the electron response model is described in detail in ref. [1]). The hadrons in the event are modeled globally, with no individual treatment of hadrons or jets. As described in ref. [6], the model of the measurement of p_T^{had} includes a resolution which is a function of the total scalar E_T observed in the event excluding the decay products of the W or the Z, and a bias on p_T^{had} which varies with the transverse momentum of the W or Z.

The p_T distribution applied to the W bosons is obtained largely from an empirical model based on the Z data. While a theoretical calculation now exists to next-to-leading order for the p_T spectra of W and Z bosons produced in $\bar{p}p$ interactions [7], the uncertainties at low p_T are still rather large. The predictions are very similar for the W and the Z however, so the p_T^Z spectrum is measured from a fit to the p_T^{ee} distribution (see Fig. 2(a)) and applied to the model for W production, taking into account the small differences predicted by theory. The correlation between rapidity and p_T is also taken from the theoretical calculation [7].

The model of the detector response to the recoiling hadrons is also studied with the aid of the Z sample by examining the momentum balance in Z events. For this study, the p_T constraint used in defining the second Z sample is not imposed. The momentum balance along the η direction is considered (η-balance $= p_\eta^{ee} + p_\eta^{had}$), where the η axis is defined by the inner bisector of the two electron directions in the transverse plane (see inset Fig. 3). Along this direction, the contribution to the resolution from p_T^{ee} is negligible, so the width of the η-balance distribution can be used to measure the resolution of the p_T^{had} measurement. In

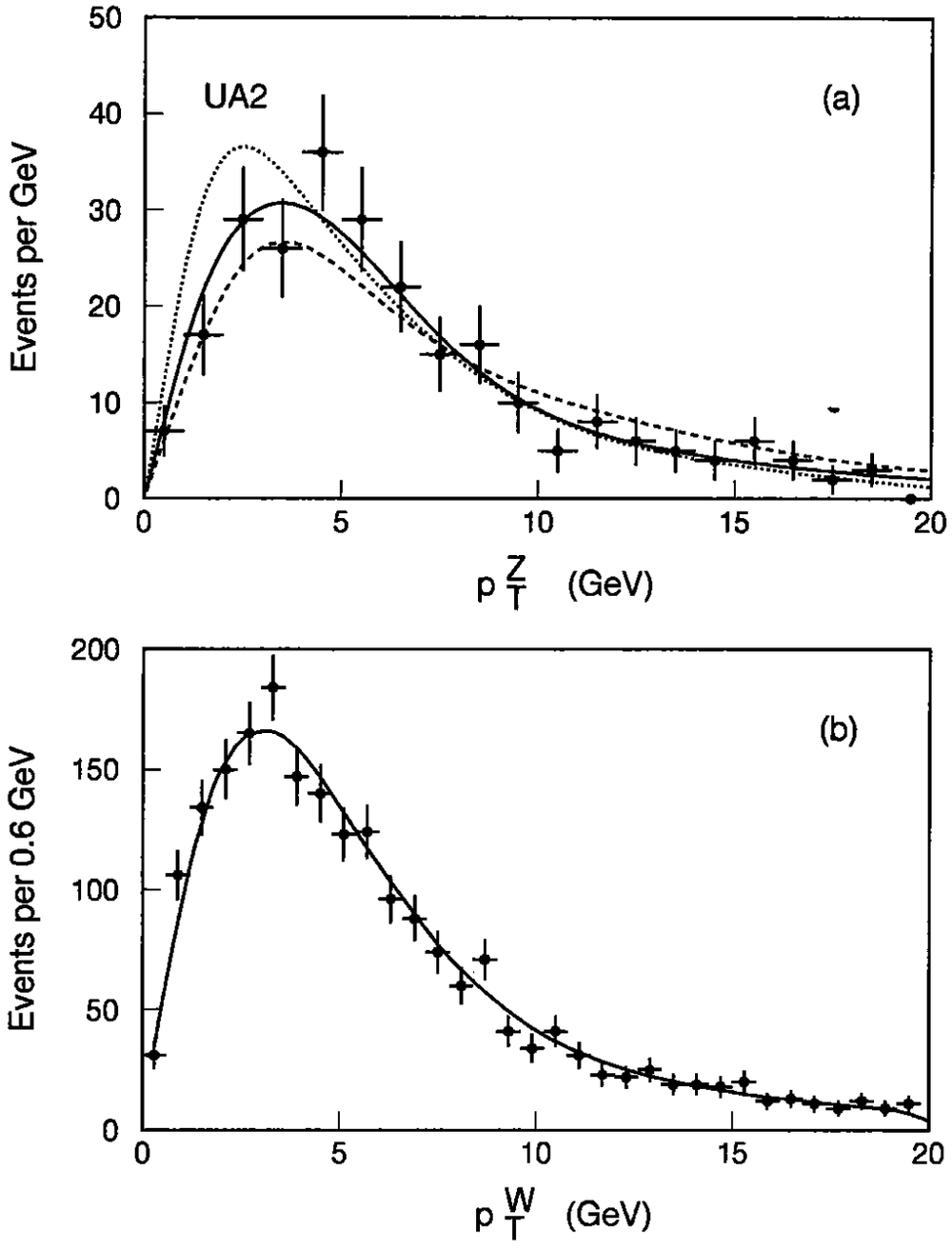

Figure 2: (a) The data for p_T^{ee} (points) and the predictions of the central model (solid) along with the soft (dotted) and hard (dashed) variations of the p_T spectrum used for systematic error studies (see text). (b) The data for $p_T^W (= -p_T^{had})$ (points) and the prediction of the central model (curve). The predictions are modified for detector acceptance and resolution.

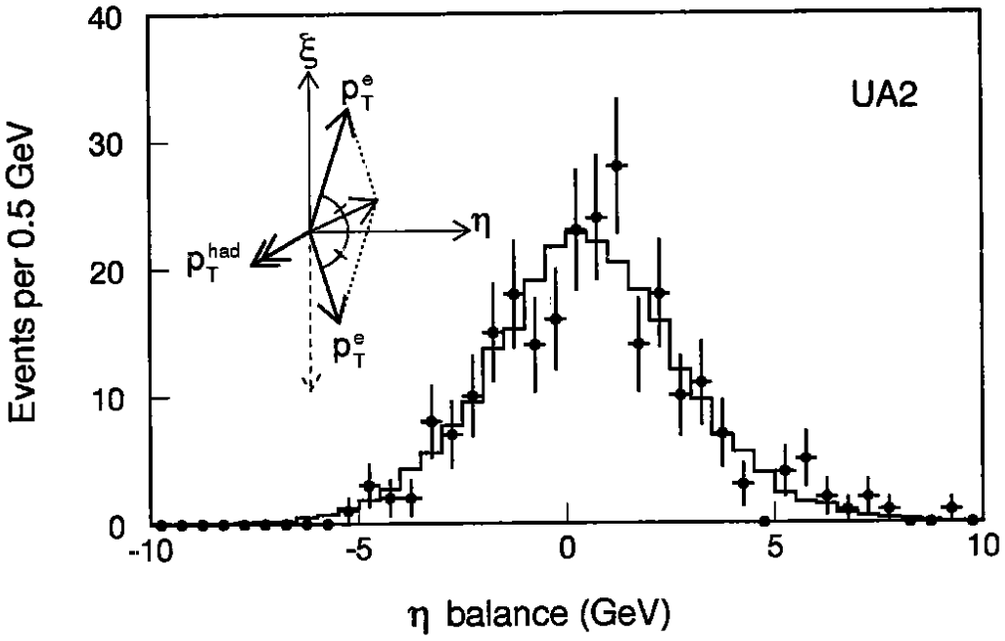

Figure 3: The momentum balance along the η axis (η-balance) in $Z \rightarrow e^+e^-$ events. The points show the data, while the histogram shows the central model.

addition, since the positive sense of the η axis is always in the direction of $\vec{p}_T^{\,Z}$, any systematic bias in the measurement of p_T^{had} manifests itself as a shift in the η-balance distribution. This distribution is shown in Fig. 3 along with the prediction of the model. The central model for the p_T^{had} measurement is obtained by tuning the resolution function and average response to give the correct width and offset in the predicted η-balance distribution.

The observed p_T^W distribution is sensitive to a combination of the true p_T^W spectrum and the measurement effects on p_T^{had}. With the parameters tuned to the Z data, the prediction of the model gives very good agreement with the observed p_T^W spectrum as shown in Fig. 2(b).

The fitting is restricted to range 60-120 GeV for the m_T fits and 30-60 GeV for the p_T^e and p_T^ν fits. The results are shown in Fig. 4 and Table 2. The three distributions are not independent, so they cannot be combined to give a more precise result. The m_T fit is used to obtain the final result because it gives the smallest statistical error as well as the smallest systematic error (see below). Meanwhile, the fits to p_T^e and p_T^ν provide a useful cross check of the measurement systematics. When statistical fluctuations and correlations are accounted for, the expected differences between the m_T fit and the p_T^e and p_T^ν fits are about 180 MeV (rms), so the three results are in good agreement. As for the Z fits, the W fits are performed with the width fixed and variable, and the fitted widths are in agreement with the Standard Model value, Γ_W=2.1 GeV.

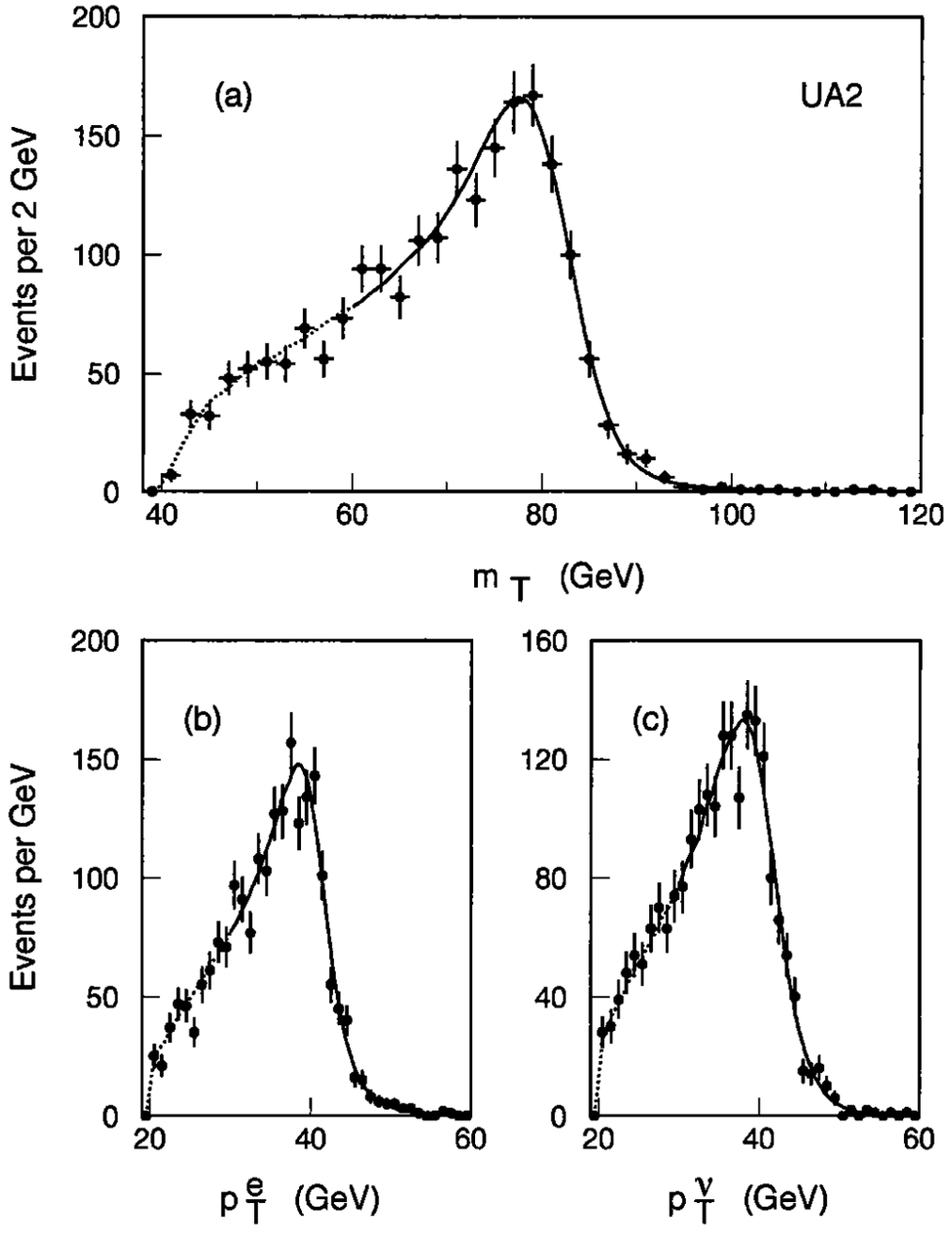

Figure 4: Fits for m_W to (a) the m_T spectrum, (b) the p_T^e spectrum and (c) the p_T^ν spectrum. The points show the data, while the curves show the fit results with the solid portions indicating the ranges over which the fits are performed.

Table 2: Results of m_W fits (statistical errors only).

	m_W(GeV)	Γ_W(GeV)
m_T	80.84 ± 0.22	2.1 (fixed)
fit	80.83 ± 0.23	2.2 ± 0.4
p_T^e	80.86 ± 0.29	2.1 (fixed)
fit	80.79 ± 0.30	2.8 ± 0.6
p_T^ν	80.73 ± 0.32	2.1 (fixed)
fit	80.70 ± 0.34	2.3 ± 0.7

4 Systematic uncertainties

The systematic effects on the m_W and m_Z measurements are summarized in Table 3. Detailed discussions of these effects are found in ref. [8]. A short description of the individual contributions follows.

Table 3: The size (in MeV) of the systematic uncertainties in measuring m_W and m_Z.

	$\delta m_W(m_T)$	$\delta m_W(p_T^e)$	$\delta m_W(p_T^\nu)$	δm_Z(central)	δm_Z(pt-con)
structure fun.	85	135	105	-	-
elec. energy resolution	75	100	75	35	35
neutrino scale	70	-	140	-	-
p_T^W and p_T^{had}	60	120	90	-	-
underlying event	30	50	-	50	50
fitting procedure	30	40	40	-	-
radiative decays	30	50	20	50	50
elec. effic. vs. p_T^e	30	40	30	-	-
$u_\parallel$ effect	25	95	350	-	-
p_T constraint	-	-	-	-	100
total syst.	160	240	420	80	130

Structure functions: For the central model, the structure function set HMRSB [9] is used. For studying systematic effects, we consider all available structure function sets which are evolved at next-to-leading order in the $\overline{MS}$ renormalization scheme (see ref. [10] and references therein). The structure functions determine a parton luminosity as a function of $\sqrt{\hat{s}}$ which distorts slightly the resonance shape of the bosons. For the Z's, this effect is represented by the constant β in equation (3), where $\beta = 0.020 \pm^{0.003}_{0.001}$ GeV^{-1}. The resulting uncertainty on the m_Z determination is less than 20 MeV and is neglected. The m_W determination is much more sensitive to the structure functions because when the acceptance is taken into account, the rapidity distribution can distort

the spectra of the transverse variables. For the m_T fits, the extreme variations are obtained with the structure function sets MT-E1 [11] (+80 MeV) and GRV [12] (-90 MeV).

If the range of the fits is extended downward, the sensitivity to structure functions increases. For example, fitting the m_T spectrum over the range $40 < m_T < 120$ GeV instead of $60 < m_T < 120$ GeV results in an increase in the structure function uncertainty from 85 MeV to 115 MeV. This motivates the change in fit range with respect to ref. [1].

Electron resolution: The energy resolution of an individual calorimeter cell is studied with test beam data and is known with a relative error of 10% for the fiducial volume used. The cell to cell gain variations contribute a constant term of $1.5 \pm 1.0\%$ to the resolution, as determined from test beam recalibration and studies on the W events themselves. An additional constant term of $1.3 \pm 0.2\%$ comes from the contribution from offset vertices. Finally, the resolution can be expressed as

$$\sigma_E/E = 17\%/\sqrt{E}(\mathrm{GeV}) \oplus 1.5\% \oplus 1.3\%, \tag{4}$$

leading to $\sigma_E/E = 3.3 \pm 0.5\%$ at $E = 40$ GeV.

Neutrino scale: To a good approximation, the scale of the p_T^ν measurement will match the scale of the p_T^e measurement, but a few small effects can contribute to an imbalance between the two which will not cancel in the mass ratio m_W/m_Z. The electron can contribute some energy to cells outside of the core which then contributes to p_T^{had}. The uncertainty on the size of this effect produces an uncertainty of ± 60 MeV in the neutrino scale. The effects of the underlying event inside the core cells contributes another uncertainty of ± 20 MeV, and the contribution of the photon to $\vec{p}_T^{\,had}$ in $e\nu\gamma$ decays of the W adds another ± 30 MeV. Taken in quadrature, the total uncertainty on $p_T^\nu - p_T^e$ is ± 70 MeV.

p_T distributions and measurement of p_T^{had}: The systematic effects due to the p_T distribution of the W are investigated by applying to the W model the hard and soft spectra shown in Fig. 2(a). These spectra are obtained by varying the parameters in the fit to the p_T^{ee} spectrum and the significance of each variation (-1.8σ and $+2.5\sigma$) is evaluated from the difference in likelihood of the p_T^{ee} prediction for the central Z sample. An additional cross check is obtained by applying the theoretical model for the p_T distribution [7] in place of the empirical model. The mass from the m_T fit changes by less than 20 MeV.

In order to understand the p_T^ν and m_T spectra, one must also consider the systematic uncertainties in the measurement of p_T^{had}. These errors are evaluated by varying in the model the resolution and average response for p_T^{had} within the ranges allowed by the statistical errors from the η-balance distribution.

The model is further constrained by requiring that the combination of true p_T^W, p_T^{had} resolution, and average p_T^{had} response predict a mean for the observed p_T^W distribution

which is consistent with the one actually measured. It is possible, for example, to increase the true p_T^W while decreasing the average response so as to maintain the same average observed p_T^W. Because of the different ways these components of the model affect the various transverse variables, constraining the p_T^W prediction reduces the systematic error on the p_T^e and p_T^ν fits, but has almost no influence on the m_T fit.

The overall sensitivity to p_T^W and p_T^{had} uncertainties gives a contribution of ± 60 MeV to the error on m_W for the m_T fit.

Underlying event: Frequently, particles from the underlying event can deposit a small amount of energy in the core cells used to measure p_T^e. The distribution of this energy is determined by examining in real W events the energy in cells not used in the electron core but at the same azimuthal position. This effect increases p_T^e by an average of 120 ± 20 MeV. For m_Z a correction of $-250 \pm 40(stat) \pm 50(syst)$ MeV is included to compensate for this increase, where the statistical error comes from the fluctuations of the underlying event effect in the small sample. In the m_W fits, the effect is already included in the model, and the uncertainty depends on which transverse variable is used, as shown in the table. For the m_T fit, the effect is, as expected, approximately half as large as for the m_Z fit.

Fitting procedure: The errors arising from the use of the numerical *pdf*'s for the m_W fits are checked by dividing the large Monte Carlo sample used in generating the *pdf*'s into many independent subsamples and fitting a fixed sample of 2000 Monte Carlo events. The resulting spread of the fit values corresponds to an uncertainty of ± 30 MeV for the m_T fits. Fits to large samples of Monte Carlo events are also used to confirm that the fits return the input value to this same precision. Fits to many Monte Carlo samples of the same size as the actual data sample verify that the statistical errors of the fits are correct.

Radiative Decays: The decays $W \to e\nu\gamma$ and $Z \to e^+e^-\gamma$ are simulated with the $O(\alpha)$ Monte Carlo program of ref. [13]. The response of the calorimeter to low energy photons is modeled with a GEANT simulation [14] which includes the effect of the preshower radiator. In order to account for the configurations where a photon lies close to an electron, the calorimeter efficiency and energy measurement are parameterized as a function of photon energy and angular separation according to a parameterization obtained by superimposing two test beam electrons where one is rescaled to the photon energy. For the systematic error evaluation, this model is compared with a naïve model where the photon is merged with the electron whenever the separation is less than 15°. For the m_Z determination, the effect of radiative decays is included as a separate correction of $+190 \pm 50$ MeV. For the m_W fits, the effect is already included in the model, and it amounts to $\sim +90$ MeV for the m_T fit, about half the size of the influence on the Z, as expected. The uncertainties in photon response give the errors indicated in the table.

The corrections beyond $O(\alpha)$ are estimated by using an exponentiation prescription [15]. The mass difference $m_W - m_Z$ changes by $+45$ MeV (-45 MeV in the m_W fit

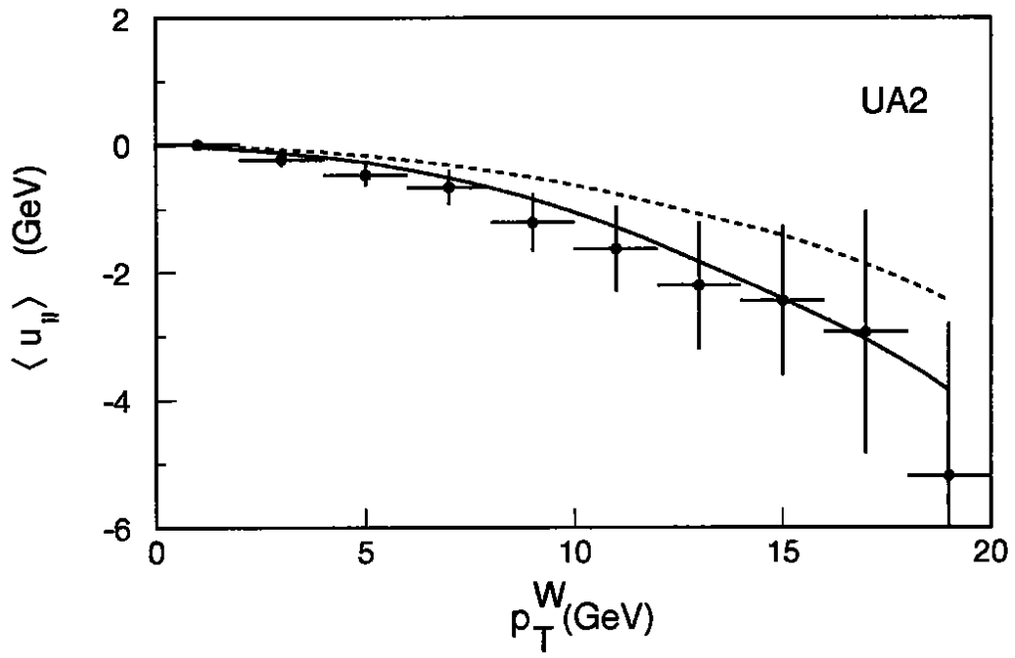

Figure 5: The average value of $u_{\parallel}$ (see text) as a function of p_T^W. The points are the data and the solid curve is the prediction of the central model. The dashed curve shows the model with the $u_{\parallel}$ dependence of the electron efficiency removed.

and -90 in the m_Z fit). These corrections are not included in the final result, but this serves to illustrate the size of higher order radiative effects.

Electron efficiency vs. p_T^e: If there is a change in electron identification efficiency with p_T^e, it can distort the transverse variable spectra and give a slight change in the measured m_W. The combined efficiency of the calorimeter, tracking and preshower requirements was studied with a combination of test beam data and W events. The change in efficiency between 40 GeV and 10 GeV is estimated to be $-5 \pm 5\%$. The influence of this uncertainty on m_W is given in Table 3, and the effect on m_Z is negligible.

Electron efficiency vs. $u_{\parallel}$: The variable $u_{\parallel}$ is defined as the component of $\vec{p}_T^{\,had}$ along the electron direction in W events. When the electron lies close to the direction of $\vec{p}_T^{\,had}$, there is a greater chance that the electron signature will be spoiled by the hadrons. Consequently, one expects a decrease in electron efficiency for large positive $u_{\parallel}$. This effect is estimated for the calorimeter signature by superimposing electrons from real W decays on W underlying events from the PYTHIA Monte Carlo [16] and running the standard pattern recognition and electron quality cuts. For the tracking and preshower, the efficiency is measured from the W data as a function of $u_{\parallel}$. The effect of applying the $u_{\parallel}$-dependent efficiency which results from these studies can be seen in Fig. 5 as a function of p_T^W (where $\vec{p}_T^{\,W} = -\vec{p}_T^{\,had}$). The tendency at large p_T^W for the average value of $u_{\parallel}$ to become increasingly negative results from a combination of kinematic effects and the loss of events with large positive $u_{\parallel}$. The uncertainties on the influence of $u_{\parallel}$

on the electron efficiency are similar to the size of the effect itself, and the resulting errors on m_W are evaluated by removing and doubling the effect in the model. The resulting uncertainties are quite large on the fits to p_T^e and p_T^ν, but cancel to first order in m_T, as shown in Table 3. This is one of the main reasons for the choice of m_T for quoting a final value for m_W.

p_T **constraint:** The m_Z measurement from the second Z sample has an additional systematic error of 100 MeV associated with the application of the p_T constraint. The uncertainty on the p_T^{had} response contributes $\sim$ 70 MeV and the treatment of the calorimeter cells assigned to the non-fiducial electron contributes $\sim$ 80 MeV.

5 Results

The combined results from the two samples of Z events give $m_Z = 91.74 \pm 0.28(\text{stat}) \pm 0.12(\text{syst}) \pm 0.92(\text{scale})$ GeV. This can be compared with the result from LEP of $m_Z = 91.175 \pm 0.021$ GeV [17]. For the W mass, the result of the m_T fit, $m_W = 80.84 \pm 0.22(\text{stat}) \pm 0.17(\text{syst}) \pm 0.81(\text{scale})$ GeV, is taken because it has the smallest errors. The scale errors from the calorimeter calibration cancel in taking the ratio m_W/m_Z aside from a residual ± 80 MeV effect of possible nonlinearities in the calorimeter energy response. In addition, some of the systematic errors contain some correlations which are taken into account. The ratio

$$m_W/m_Z = 0.8813 \pm 0.0036(\text{stat}) \pm 0.0019(\text{syst}) \tag{5}$$

can be multiplied by the LEP value of m_Z to give a more precise value for the W mass:

$$m_W = 80.35 \pm 0.33(\text{stat}) \pm 0.17(\text{syst}) \text{ GeV}. \tag{6}$$

Combining the statistical and systematic errors, one obtains $m_W = 80.35 \pm 0.37$ GeV. Using the Sirlin [18] convention $\sin^2\theta_W \equiv 1 - {m_W}^2/{m_Z}^2$, equation (5) implies

$$\sin^2\theta_W = 0.2234 \pm 0.0064 \pm 0.0033. \tag{7}$$

This value is in agreement with the result derived from low energy data $\sin^2\theta_W = 0.2309 \pm 0.0029(\text{stat}) \pm 0.0049(\text{syst})$ [19].

The CDF experiment has measured $m_W = 79.91 \pm 0.39$ GeV [2], which is in good agreement with the present measurements. When the results of UA2 and CDF are combined the results are $m_W = 80.14 \pm 0.27$ GeV and $\sin^2\theta_W = 0.2274 \pm 0.0052$.

Within the Standard Model, the ratio m_W/m_Z is determined at the Born level from the parameters α, G_μ, and m_Z. Radiative corrections can modify this prediction significantly. In the minimal Standard Model, these corrections depend strongly (quadratically) on the mass of the top quark (m_{top}) [20] and weakly (logarithmically) on the mass of the Higgs boson (m_H). Consequently, the measurement of m_W/m_Z can be used to place some (model dependent) bounds on m_{top}. This is illustrated in Fig. 6 [21]. From the UA2 result alone, one can conclude that $m_{top} = 160 \pm^{50}_{60}$ GeV for m_H=100 GeV, and $m_{top} < 250$ GeV at the 95% confidence level for $m_H < 1$ TeV. The combined results of UA2 and CDF yield $m_{top} = 130 \pm^{40}_{50}$ for m_H=100 GeV and $m_{top} < 215$ GeV at the 95% confidence level for $m_H < 1$ TeV (the

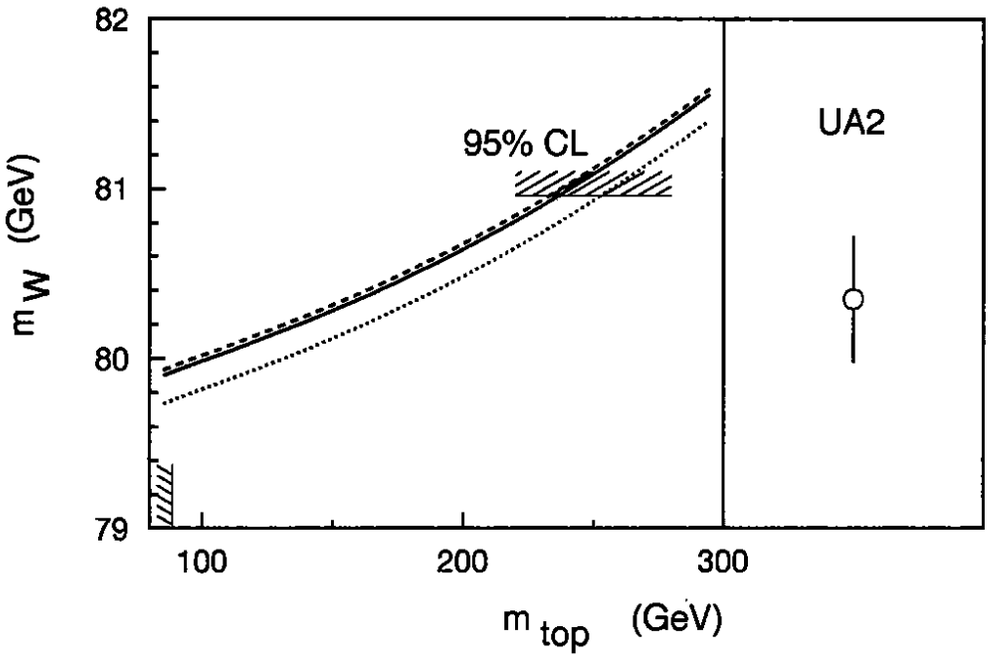

Figure 6: The final result for m_W is compared with the Standard Model predictions for m_W as a function of m_{top} and m_H[21]. The dotted, solid and dashed curves correspond to Higgs masses of 50 GeV, 100 GeV, and 1000 GeV, respectively.

calculations [21] are no longer valid for $m_H \gtrsim 1$ TeV). Note that direct searches place a limits of $m_{top} > 89$ GeV [22] and $m_H > 48$ GeV [23].

The LEP measurements of mass, width, and asymmetries at the Z pole can be combined, within the assumptions of the minimal Standard Model, to give a prediction of the W mass of $m_W = 80.14 \pm 0.19$ GeV [17]. Similarly, the $\sin^2\theta_W$ measurement from neutrino scattering [19] can be combined with m_Z from LEP to give a minimal Standard Model prediction of $m_W = 79.96 \pm 0.30$ GeV. Both of these indirect determinations are in excellent agreement with the collider measurements of m_W.

6 Conclusions

The final data sample of the UA2 experiment has been used to make a direct determination of the ratio of W and Z masses. The result is

$$m_W/m_Z = 0.8813 \pm 0.0036(\text{stat}) \pm 0.0019(\text{syst}). \tag{8}$$

In combination with the m_Z measurement from LEP, this gives

$$m_W = 80.35 \pm 0.33(\text{stat}) \pm 0.17(\text{syst}) \text{ GeV}. \tag{9}$$

The result agrees well with a similar determination from CDF and with Standard Model predictions based on LEP data. Within the minimal Standard Model, this measurement of m_W implies that $m_{top} < 250$ GeV at the 95% confidence level.

Acknowledgements

Many theory colleagues have provided us with essential assistance in the form of discussions and computer programs. In particular, we would like to thank G. Altarelli, P. Arnold, R. Kleiss and J. Stirling.

The technical staff of the institutes collaborating in UA2 have contributed substantially to the construction and operation of the experiment. We deeply thank them for their continuous support. The experiment would not have been possible without the very successful operation of the improved CERN $\bar{p}p$ Collider, whose staff and coordinators we sincerely thank for their collective effort.

Financial support from the Schweizerischen Nationalfonds zur Förderung der Wissenschaftlichen Forschung to the Bern group, from the UK Science and Engineering Research Council to the Cambridge group, from the Bundesministerium für Forschung und Technologie to the Dortmund and Heidelberg groups, from the Australian Research Council, the CRA Pty Ltd, and the Victorian Education Foundation to the Melbourne group, from the Institut National de Physique Nucléaire et de Physique des Particules to the Orsay group, from the Istituto Nazionale di Fisica Nucleare to the Milano, Pavia, Perugia and Pisa groups and from the Institut de Recherche Fondamentale (CEA) to the Saclay group are acknowledged.

References

[1] UA2 Collab., J. Alitti *et al.*, *Phys. Lett.* **B241** (1990) 150.

[2] CDF Collab., F. Abe, *et al.*, *Phys. Rev. Lett.* **65** (1990) 2243;
Phys. Rev. **D43** (1991) 2070.

[3] UA2 Collab., J. Alitti, *et al.*, *A Measurement of the W and Z Production Cross Sections and a Determination of* Γ_W *at the CERN* $\bar{p}p$ *Collider,* CERN PPE/91-162, accompanying letter.

[4] UA2 Collab., J. Alitti *et al.*, *Z. Phys.* **C47** (1990) 11.

[5] F.A. Berends, Z^0 *Physics at LEP1*, vol 1, p. 89, CERN 89-08.

[6] UA2 Collab., J. Alitti *et al.*, *Z. Phys.* **C47** (1990) 523.

[7] P.B. Arnold and R.P. Kauffman, *Nucl. Phys.* **B349** (1991) 381.

[8] G. Unal, thesis, Université de Paris-Sud, Centre D'Orsay, LAL 91-13, (1991).

[9] P.N. Harriman, A.D. Martin, R.G. Roberts, and W.J. Stirling, *Phys. Rev.* **D42** (1990) 798;
Phys. Lett. **B243** (1990) 421.

[10] H. Plothow-Besch, *Parton Density Functions*, Proceedings of the 3rd Workshop on Detector and Event Simulation in High Energy Physics (Amsterdam, April 1991).

[11] J.G. Morfín and W.K. Tung, Fermilab Preprint Fermilab-PUB-90/74.

[12] M. Glück, E. Reya and A. Vogt, *Z. Phys* **C48** (1990) 471.

[13] F.A. Berends and R. Kleiss, *Z. Phys* **C27** (1985) 365;
F.A. Berends, R. Kleiss, J.P. Revol, and J.P. Vialle, *Z. Phys.* **C27** (1985) 155.

[14] R. Brun, *et al.*, GEANT3, CERN Report DD/EE/84-1 (1989).

[15] R. Kleiss, private communication.

[16] H. Bengtsson and T. Sjöstrand, *The Lund Monte Carlo for Hadronic Processes*, LUTP 87-3, UCLA 87-001
T. Sjöstrand and M. Bengtsson, *The Lund Monte Carlo for jet fragmentation and e^+e^- physics*, LUTP 86-22.

[17] J. Carter, summary talk at Lepton-Photon Symposium and Int. Europhysics Conference on High Energy Physics (Geneva, July-August 1991).

[18] A. Sirlin, *Phys. Rev.* **D22** (1980) 971.

[19] G.L. Fogli, D. Haidt, *Z. Phys.* **C40** (1988) 379.

[20] M. Veltman, *Nucl. Phys.* **B123** (1977) 89.

[21] W. Hollik, G. Burgers, *Z^0 Physics at LEP1*, volume 1, CERN 89.08.

[22] K. Sliwa, in *High Energy Hadron Interactions*, proceedings of the XXVth Rencontres de Moriond, Les Arcs, France, edited by J. Tran Thanh Van (Editions Frontieres, Gif-sur-Yvette, 1990).

[23] ALEPH Collab., D. Decamp *et al.*, preprint CERN-PPE/91-19;
DELPHI Collab., P. Abreu *et al.* preprint CERN-PPE/90-163;
OPAL Collab., M.Z. Akrawy *et al.*, *Phys. Lett.* **B253** (1991) 511;
L3 Collab., B. Adeva *et al.*, L3 preprint #24, December 1990.